Modelling and identification of delamination defects

Anita Orlowska, Jan Holnicki-Szulc, Przemyslaw Kolakowski
Institute of Fundamental Technological Research, Smart Technology Centre,
Świętokrzyska 21, 00-049 Warszawa
e-mail: aorlow@ippt.gov.pl
http://ippt.gov.pl

ABSTRACT

A software tool for signal processing in health monitoring of structural elements composed of laminated layers is presented. This new approach to the damage (delamination) identification problem is based on analysis of perturbation in low-frequency vibration responses. Generalizing the so-called VDM (Virtual Distortion Method) approach for dynamic problems, a dynamic influence matrix D concept will be introduced. Pre-computing of the time-dependent matrix D allows for decomposition of the dynamic structural response into components caused by external excitation in undamaged structure (the linear part) and components describing perturbations caused by the internal defects (the non-linear part). As a consequence, analytical formulae for calculation of these perturbations and the corresponding gradients can be derived. The physical meaning of the so-called *virtual distortions* used in this paper can be explained with the help of externally induced strains (non-compatible in general, e.g. caused by piezoelectric transducers, similarly to the effect of non-homogeneous heating). The compatible strains and self-equilibrated stresses are structural responses to these distortions. Assuming possible locations of all potential defects in advance, an optimisation technique with analytically calculated gradients could be applied to solve the problem of the most probable location of defects.

INTRODUCTION

The damage detection systems based on array of piezoelectric transducers sending and receiving strain waves are intensively discussed by researchers recently. The signal-processing problem is the crucial point in this concept and a neural network based method is one of the most often suggested approaches to develop a numerically efficient solver for this problem.

An alternative way for these techniques is the VDM approach. The software tool based on this method can be dedicated for different kind of damage, also for delamination identification problem, which will be discussed below.

The numerical results for delamination identification will be presented, both for the static and dynamic VDM approach.

This paper is a continuation of the paper [5].

VDM STATIC APPROACH IN DELAMINATION MONITORING

We shall pose the optimisation problem of structural damage identification (constraining ourselves temporarily to the static case) within the framework of the Virtual Distortion Method (cf. [4]). Let us minimise the following function:

$$\min \sum_{A} \left(\varepsilon_A^M - \varepsilon_A \right)^2 \tag{1}$$

which can be interpreted as an average departure of the total structural strain $\boldsymbol{\varepsilon}_A$ from the in-situ measured strain $\boldsymbol{\varepsilon}_A^M$ in damaged locations A. Taking advantage of the VDM formulation we can decompose the strain $\boldsymbol{\varepsilon}_A$ into two parts:

$$\varepsilon_A = \varepsilon_A^L + \varepsilon_A^R = \varepsilon_A^L + \sum_A D_{Ai} \varepsilon_i^o \tag{2}$$

where $\boldsymbol{\varepsilon}_A^L$ denotes the response of undamaged structure, $\mathbf{D}$ is the influence matrix and $\boldsymbol{\varepsilon}^o$ is the virtual distortion vector. As the component $\boldsymbol{\varepsilon}_A^L$ is constant for a given external load, the so-called residual strain component $\boldsymbol{\varepsilon}_A^R$ may only be varying in the optimisation process with the virtual distortion $\boldsymbol{\varepsilon}^o$ as the design variable.

We shall measure the structural damage in each member i with the help of the coefficient μ_i i.e. with the ratio of cross-sectional areas of a damaged member to the undamaged one. Consequently we have to impose appropriate constraints on this coefficient. As we examine the physical process of deterioration of the member cross-section we are interested in such μ_i, which complies with the following constraints:

$$0 \le \mu_i \le 1 \quad \text{i.e.} \quad 0 \le \frac{\varepsilon_i - \varepsilon_i^o}{\varepsilon_i} \le 1 \tag{3}$$

For delamination problems the coefficient μ will finally (after optimisation) take only two values: 0 (delamination) or 1 (full connection).

The gradients of the objective function and the constraints are expressed in terms of the design variable $\boldsymbol{\varepsilon}^o$ as follows:

$$\nabla f = \frac{\partial f}{\partial \varepsilon_k^o} = -2 \sum_A D_{Ak} \left(\varepsilon_A^M - \varepsilon_A \right) \tag{4a}$$

and

$$N = n_{kl} = \frac{\partial g_l}{\partial \varepsilon_k^o} = \frac{\delta_{lk}\varepsilon_l - D_{lk}\varepsilon_l^o}{(\varepsilon_l)^2} \tag{4b}$$

In order to solve the damage identification problem posed by (1) and (3) the Gradient Projection Method (cf. [1], [2], [3]) can be used as optimisation tool. The Gradient Projection Method is based on the idea of projecting the search direction (i.e. the direction in which the objective function value decreases) into the subspace tangent to the active constraints. For the case of linear constraints the optimisation problem can be posed in the following way:

$$\min\ f(x) \tag{5}$$

subject to:

$$g_j(x) = \sum_{i=1}^{n} n_{ji} x_i - b_j \geq 0, \quad j = 1,...,n_g \tag{6}$$

where $n_{kl} = \frac{\partial g_l}{\partial x_k}$ i.e. the gradients of the constraints are stored column-wise. Subscripts *i* and *k* run through the number of design variables *n* whereas subscripts *j* and *l* run through the number of constraints n_g.

If we select only the *r* active constraints then the constraints may be written as follows:

$$g_a = N^T x - b = 0 \tag{7}$$

where the matrix **N** stores gradients of the constraints in columns.

NUMERICAL EXAMPLE – STATIC CASE

In the modelling of contact layer the following conditions have been imposed on the pair of inclined elements (left and right) and on the transversal one in each delaminated cell "*i*" (cf. Fig.1):

- in the case of transversal compression in delaminated cell "*i*":

$$\varepsilon_{iR}^0 = \varepsilon_{iR} \quad \varepsilon_{iL}^0 = \varepsilon_{iL}$$
$$\varepsilon_{iN}^0 = \varepsilon_{iN} \tag{8}$$

- in the case of non-compressive transversal interactions in delaminated cell "*i*":

$$\varepsilon_{iR}^0 = \varepsilon_{iR} \quad \varepsilon_{iL}^0 = \varepsilon_{iL}$$
$$\varepsilon_{iN}^0 = 0 \tag{9}$$

where

$$\varepsilon_{iR} = \varepsilon_{iR}^L + \sum_{j,k} D_{iR,jk}\varepsilon_{jk}^0 \ ; \ \varepsilon_{iL} = \varepsilon_{iL}^L + \sum_{j,k} D_{iL,jk}\varepsilon_{jk}^0$$
$$\varepsilon_{iN} = \varepsilon_{iN}^L + \sum_{j,k} D_{iN,jk}\varepsilon_{jk}^0 \ ; \ k = R, L, N \tag{10}$$

and $D_{iR,jk}$, $D_{iL,jk}$, $D_{iN,jk}$ denote influence vectors describing strains generated in elements: right, left and normal in the cell "*i*" induced due to unit virtual distortion generated in element "*jk*".

The above conditions leads to the following effects modelling the contact problem in the gap generated due to delamination:

- in the case of transversal compression in delaminated cell "*i*" the shear forces vanish in the contact layer,
- in the case of non-compressive transversal interactions in delaminated cell "*i*" the shear forces as well as the transversal forces vanish.

The sets of equations (8), (9) allows determination of virtual distortions modelling shear movement and transversal gap development along the contact layer. The resultant strains in contact elements take the form (10).

The algorithm for the contact problem analysis in delaminated layer is shown in Table 1.

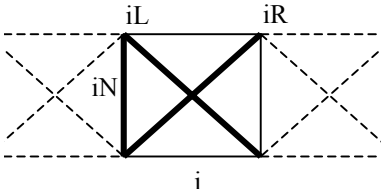

Fig.1 Notation used in description of the contact layer.

Table 1. The algorithm for the contact problem analysis in delaminated layer.

INITIALIZATION

Determine:

Linear response undamaged structure ε_{ik}^{L}

influence matrix: $D_{im,jk} \quad m,k = R,L,N$

damage vector $\mu_{iR}, \mu_{iL}, \mu_{iN}$

FOR EACH TIME STEP t:

Assuming transversal compression in delaminated zone equations (8), (10) allow to determine associated virtual distortions (cf.(8)),what leads to the following system of equations Ax=b, where:

$$A = \begin{bmatrix} (1-\mu_{iR})(D_{iR,jR} - \delta_{ij}) & (1-\mu_{iL})D_{iR,jL} \\ (1-\mu_{iR})D_{iL,jR} & (1-\mu_{iL})(D_{iL,jL} - \delta_{ij}) \end{bmatrix} \; ; B = \begin{bmatrix} -(1-\mu_{iR})\varepsilon_{iR}^{L} \\ -(1-\mu_{iL})\varepsilon_{iL}^{L} \end{bmatrix};$$

Update responses for each vertical element in delaminated area:

$\varepsilon_{iN} = \varepsilon_{iN}^{L} + \sum_{j} D_{iN,jR}\varepsilon_{jR}^{0} + \sum_{j} D_{iN,jL}\varepsilon_{jL}^{0}$

and check if :

$\varepsilon_{iN} \geq 0$

NO

YES

In the case of non-compressive transversal interactions determine associated virtual distortions from equations (9), (10), what leads to the following system of equations Ax=b, where:

$$A = \begin{bmatrix} (1-\mu_{iR})(D_{iR,jR} - \delta_{ij}) & (1-\mu_{iL})D_{iR,jL} & (1-\mu_{iN})D_{iR,jN} \\ (1-\mu_{iR})D_{iL,jR} & (1-\mu_{iL})(D_{iL,jL} - \delta_{ij}) & (1-\mu_{iNi})D_{iL,jN} \\ (1-\mu_{iR})D_{iN,jR} & (1-\mu_{iL})D_{iN,jL} & (1-\mu_{iN})(D_{iN,jN} - \delta_{ij}) \end{bmatrix}; \quad B = \begin{bmatrix} -(1-\mu_{iR})\varepsilon_{iR}^{L} \\ -(1-\mu_{iL})\varepsilon_{iL}^{L} \\ -(1-\mu_{iN})\varepsilon_{iN}^{L} \end{bmatrix};$$

Update responses for each element:

$$\varepsilon_{im} = \varepsilon_{im}^{L} + \sum_{j,k} D_{im,jk}\varepsilon_{jk}^{0} \quad ; \; \varepsilon_{A} = \varepsilon_{A}^{L} + \sum_{j,k} D_{A,jk}\varepsilon_{jk}^{0}$$

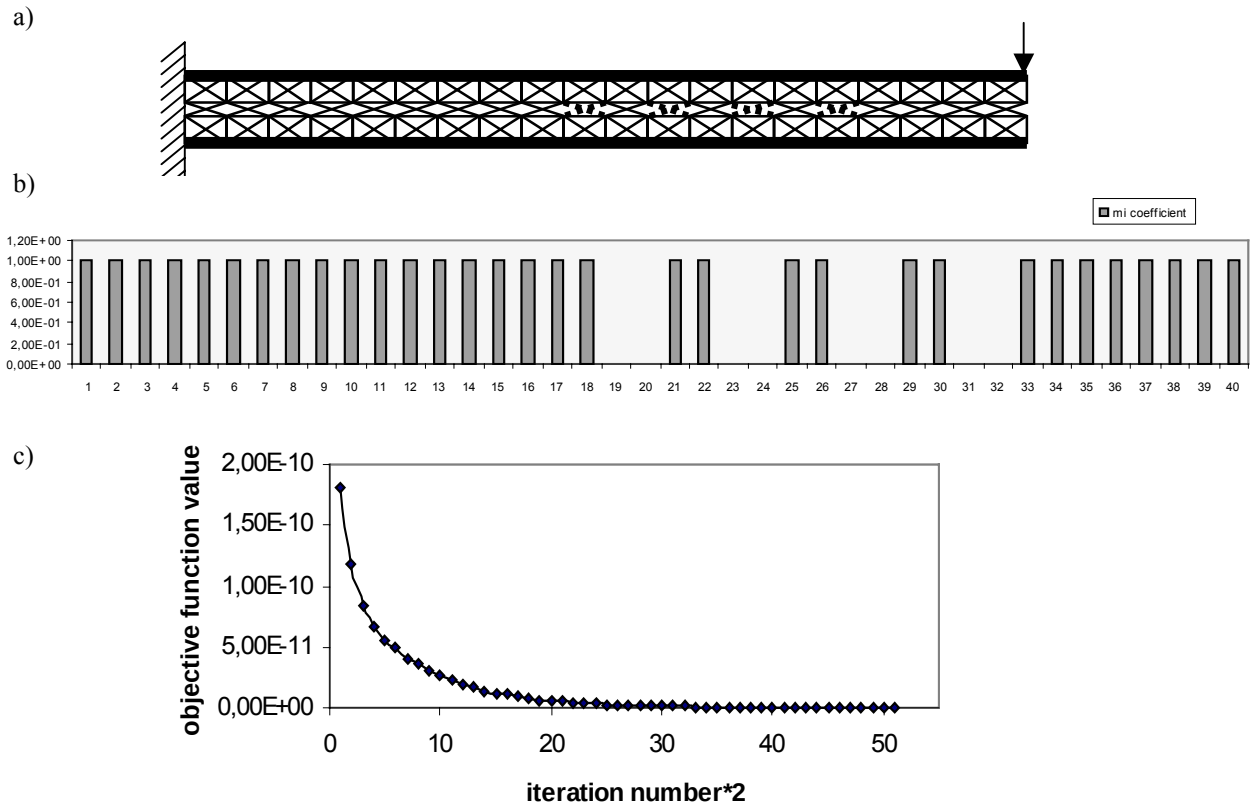

Fig.2 (a) Cantilever truss structure consisting of 2 outer layers joined by the inner layer, which exhibits delamination in few locations (dashed lines). Sensors (elements able to detect strain) are placed in upper and lower horizontal members marked by bold lines. Static vertical force was applied at free end to identify the delamination defects.(b) virtual distortions and damage coefficient values obtained during optimization process. (c) optimization routine progress.

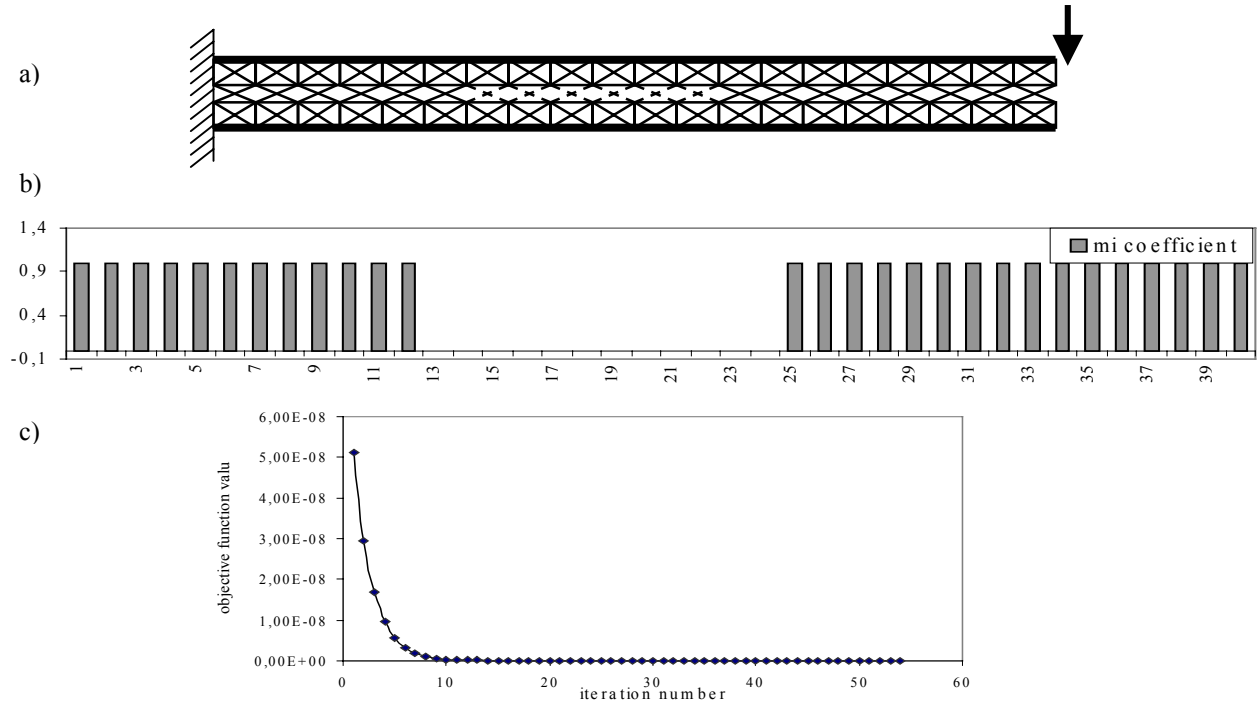

Fig.3. (a) Extensive delamination case. Sensors are marked by bold lines. Static vertical force was applied at free end to identify the delamination defects.(b) Damage coefficient values obtained in optimization process. (c) Optimization routine progress.

A simple truss model has been used demonstrating the problem of identification of delamination zone. The delaminated region has been modelled as a very thin layer (composed of truss elements also) placed between two thick layers.
Numerical tests have been done for different delamination zone positions and sizes. Optimization routine was successful in finding defects, but large number of sensors was used, especially in the case of full delamination effect.

DYNAMIC CASE

The problem of identification of delaminations defined as a static problem leads to multi-sensor *observability*, which was demonstrated above. Let us demonstrate now, that the same problem, defined as a dynamic one, allows us to use only few sensors. Assuming impact excitation (generated by an actuator), transmitted along the beam and measured by a sensor located in a distance, the inverse dynamic analysis has to be performed in order to identify locations and intensities of defects. The Dynamic Virtual Distortion Method (Ref. 4), which is based on assumption that the virtual distortions depend on time, can be applied as the solver of the current identification problem. Both the structural response and influence matrix are time-dependent, and the formula for measured strain development (2) takes now the following form:

$$\varepsilon_A(t)=\varepsilon_A^L(t)+\varepsilon_A^R(t)=\varepsilon_A^L(t)+\sum_{\tau=0}^{t}\sum_{j,k} D_{A,jk}(t-\tau)\varepsilon_{jk}^0(\tau) \qquad (11)$$

It is important to note, that time-dependent influence matrix is obtained for unit impulse excitations applied in time instant t=0 (it means that excitation has non-zero value only for one time step). The unit impulse excitation can be supplied in form of initial velocity conditions: $V(0)=\frac{P\Delta t}{m}$, where P denotes compensative force corresponding to locally generated unit virtual distortion impulse $\varepsilon^0=1$, Δt denotes the integration time step, and *m* - the mass concentrated in the loaded element. Having the influence matrix $D_{A,jk}(t)$ (in the case of only one sensor $D_{A,jk}(t)$ describes strain in observable element A, for each possible location of compensative forces) we can calculate the superposition of linear, time-dependent structural responses.

In case of non-extensive delamination (e. g. one-section) the normal forces in the contact layer have non-zero values. In case of extensive delamination there can appear the efect of an open gap, when the normal forces in the contact layer (in delaminated zone) vanish. Such situation is illustrated in Fig. 4. The damage was localized in the middle part of the structure (elements marked as dotted lines) and delamination crack size was near 1/3 length of the beam. As it is shown in Fig. 4c, when the strains for a vertical element placed in the damaged region (bold line) become positive, virtual distortions β_i^0 take non-zeroes values (it's the open gap situation).

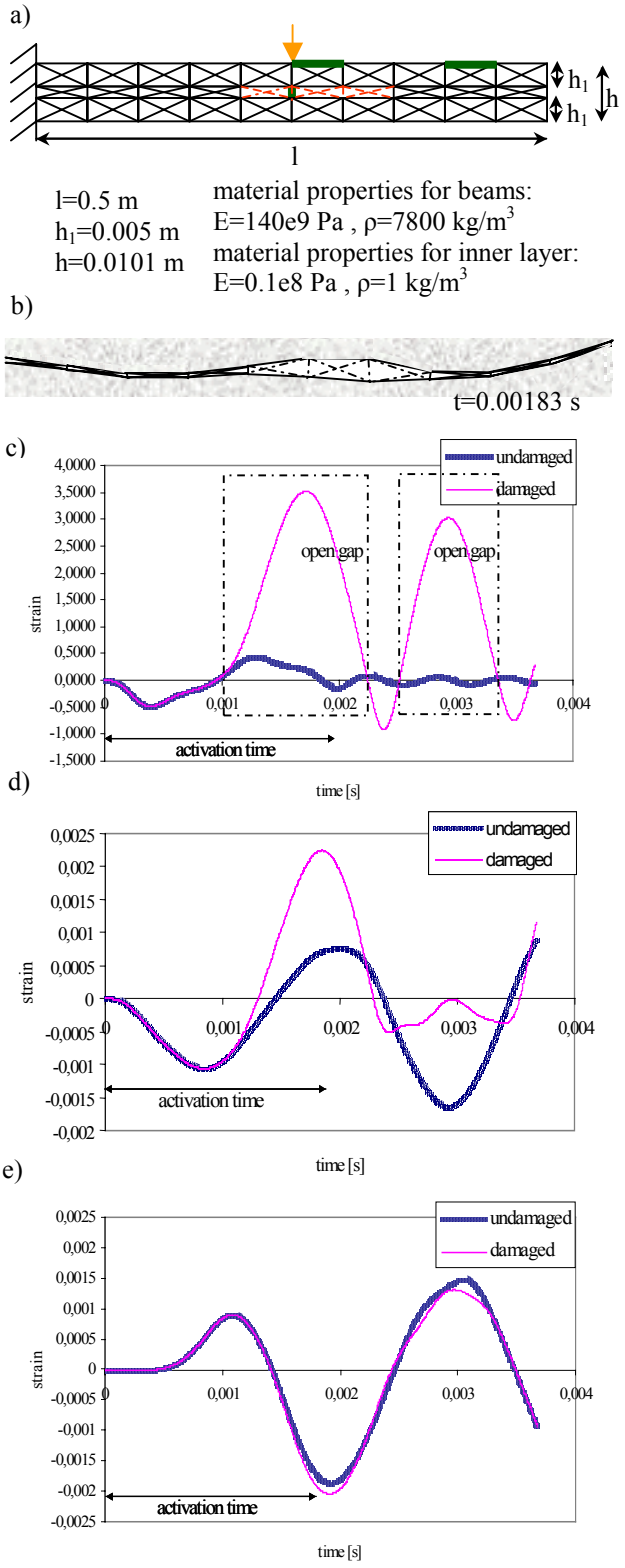

Fig.4 Extensive delamination case. (a) Numerical model (dotted lines-damage, bold lines-sensors, arrow-excitation point), (b) delaminated layer behaviour for the time moment t=0.00183 s, (c) responses of the undamaged and damaged structure for vertical element localized inside the delaminated zone, (d) responses for the sensor placed near the excitation point, (e) responses for the sensor placed near the free end of the structure.

The inverse analysis leads to minimisation of the objective function describing differences between the measured response ε_A^M and the modelled one ε_A (expressed by Eq. 8). Finally, the defect identification problem takes the following form:

$$\min \sum_t (\varepsilon_A^M(t) - \varepsilon_A(t))^2 \tag{12}$$

subject to the following constraints, where μ is defined by the time-dependent version of the formula (3):

$$0 \le \mu_i \le 1 \tag{13}$$

132-element truss-structure model has been used in the dynamic case presented below (Fig.6). The natural frequencies for this model (without damage) were:

1) 28.032
2) 154.73
3) 381.83
4) 666.16
5) 1004.3
6) 1396.4

The natural frequencies for one damaged section are presented in table 2.

Table 2: Natural frequencies for damaged structure.

damaged section number	I natural frequency	II natural frequency	III natural frequency	IV natural frequency	V natural frequency	VI natural frequency
1	28.012	153.76	378.52	661.83	1001.4	1395.6
2	27.916	149.81	371.58	661.58	1004.3	1391.9
3	27.913	151.16	380.98	660.13	985.83	1389.4
4	27.922	153.08	378.87	650.50	1003.7	1383.3
5	27.936	154.44	371.70	665.24	985.54	1391.2
6	27.955	154.68	373.54	654.86	998.46	1382.2
7	27.976	154.09	380.74	645.13	991.33	1395.6
8	27.999	153.59	380.55	663.65	982.6	1372.3
9	28.018	153.82	377.23	661.80	1004.0	1393.1
10	28.024	153.93	374.46	645.24	970.94	1359.8

The frequency change in case of small, one-section damage which is inserted in different location along the contact layer, is small for I and II natural frequency. More evident changes occur for frequencies from III up to VI natural frequency of the structure .

Let's discuss the case of damage located in section 5 (Fig. 5). The excitation signal is one period of the sinusoidal wave of the frequency corresponding to IV natural frequency of the undamaged structure (666.16 Hz). The first gradient values are very important for the optimization routine. For the one-section delamination damage case, the gradient disturbance has a localized character. It means that optimal sensor location is near the damaged section (first gradients for sensors placed in long distance from damage are flat).

There will be two cases of sensor location compared. In the case of one sensor (Fig. 5) placed near the free end of the structure, gradient values at the begining of the optimization process are at the same level (do not show that damage is localized in section 5). After 80 iterations the goal function value is approaching zero but still decreasing. As shown in Fig. 8b the damage coefficient for section 5-th is also near zero. It seams to be promising for identification but very time-consuming.

In the case of three sensors the first gradient with index 5 is at higher level than others, and we have quite good identification results already after 20 iterations.

The computation of gradients for this case was done for every of the three sensors (in every optimization iteration). The way for doing computation faster is to evaluate the most possible location of damage (using results from a few sensors) and compute gradients only for the sensor with the biggest difference between the damaged and.undamaged response.

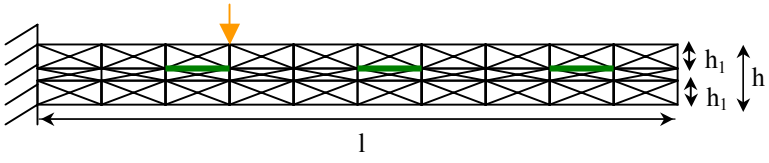

l=0.5 m
h_1=0.005 m
h=0.0101 m

material properties for beams:
E=140e9 Pa , ρ=7800 kg/m^3
material properties for inner layer:
E=140e9 Pa , ρ=1 kg/m^3

Fig.5 Truss-structure model (not scaled) with the sensors (bold lines) and the excitation point (arrow) .

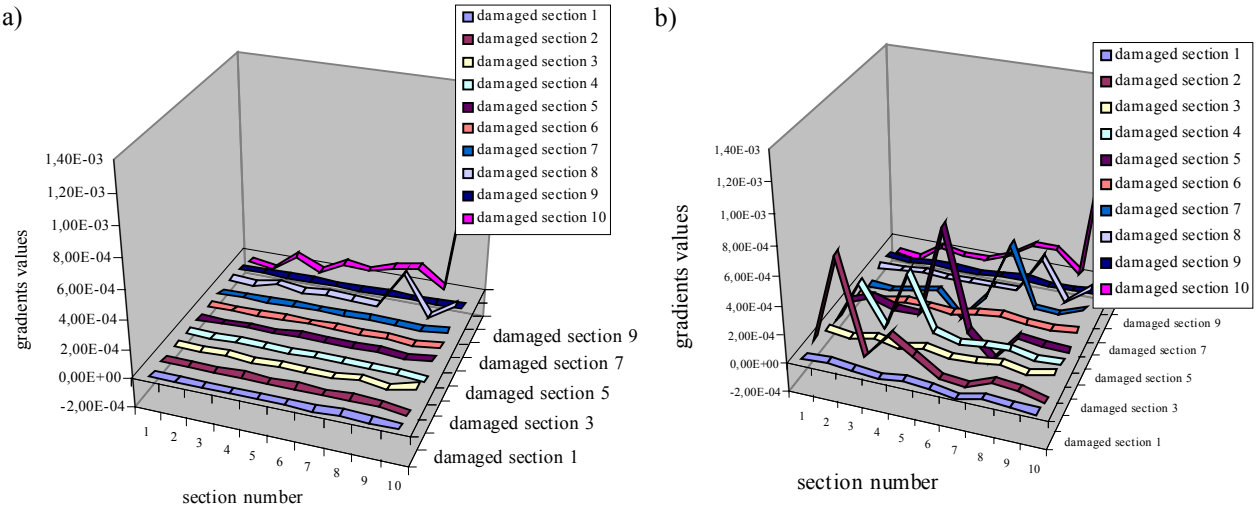

Fig. 6 Gradient values (one-section damage case), a) for one sensor placed near the free end of the structure, b) for three sensors.

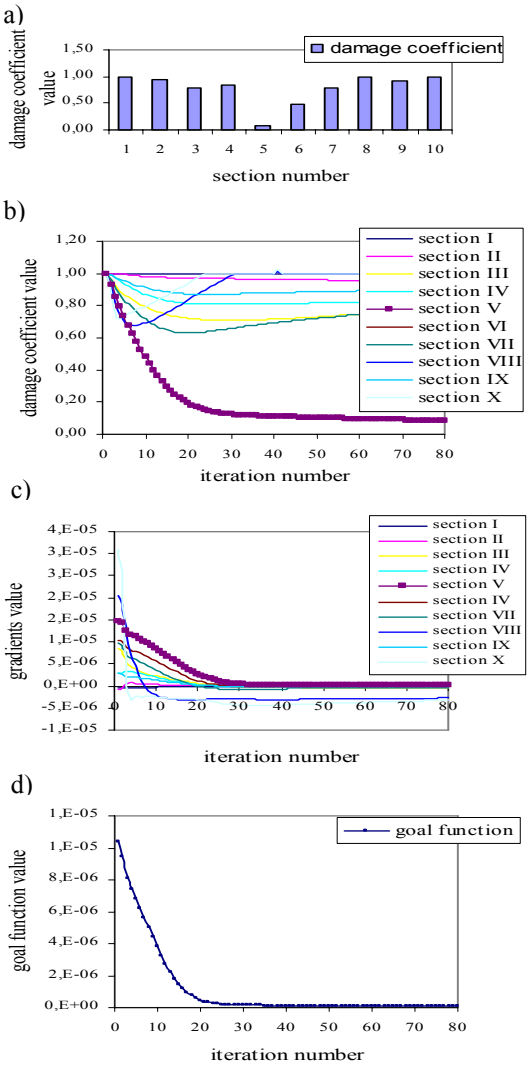

Fig. 7 Identification results for one sensor. a) Damage coefficient values at last iteration, b) damage coefficient values for each iteration, c) evolution of gradients, d) goal function changes .

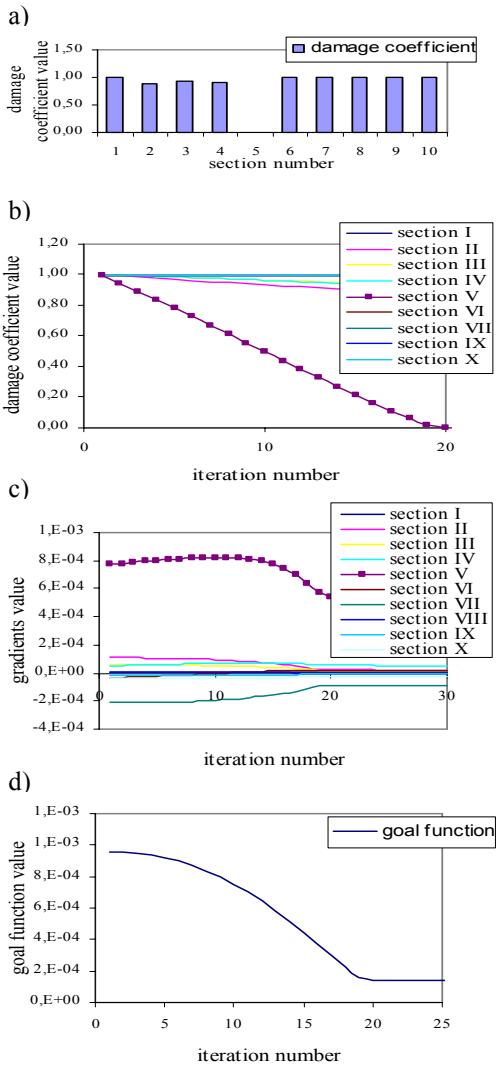

Fig. 8 Identification results for three sensors. a) Damage coefficient values at last iteration, b) damage coefficient values for each iteration, c) evolution of gradients, d) goal function changes.

REAL-TIME DETECTION OF DELAMINATION

The previously discussed cases (the static and the dynamic one) can be considered as *aposteriori* testing detecting and identifying already existing delaminations. However, in many applications a real-time health monitoring is the challenge. Heaving sensor system mounted permanently to the operating structure, the damage detection "in motion" seams to be feasible. Let us discuss the case of our testing beam under steady-state excitation (380 Hz) with delemination (in section No.5) generated in the time step 500 (Fig. 9). The strain evolution in the series of elements next to the contact layer is demonstrated.

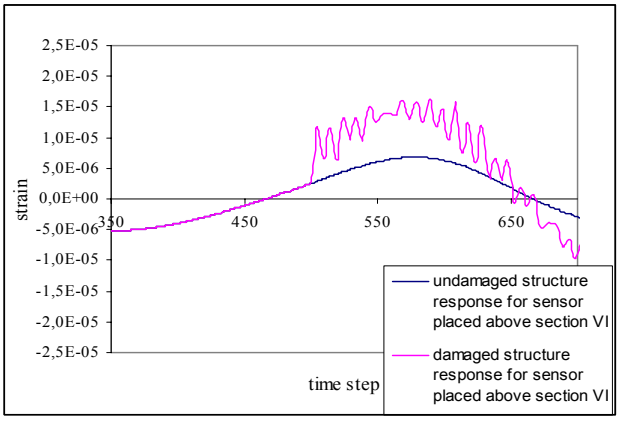

Fig.9 Responses (damaged and undamaged) for sensor placed above section VI.

a)

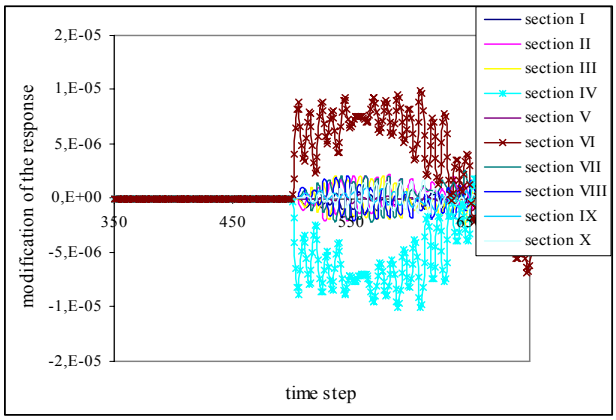

b)

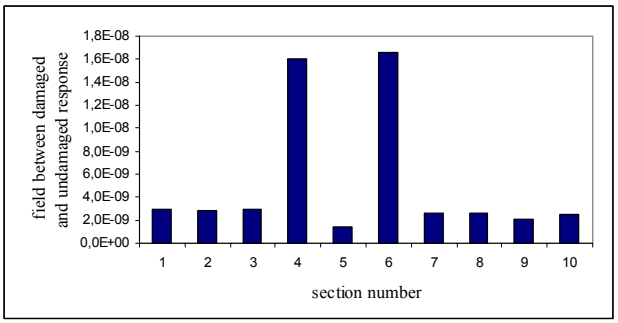

Fig.10 a) Modification of the response due to the delamination in 5-th section, b) field between damaged and undamaged response.

Extracting wave propagation due to the delamination effect (neglecting response to external excitation) the strain evolution shown in Fig.10 can be obtained.

Two algorithms for automatic identification of delamination based on the above results (Fig. 10) can be proposed. The first, a simple one, but requiring relatively dens distribution of sensors and the second one, more sophisticated but requiring only one or few sensors. The first algorithm can be based on determination of the pair of two sensors with maximal average signal (cf. Fig.10b demonstrating the field under curves from the Fig. 10a). The delamination area is located in-between these maximally loaded sensors. The example with more extended delamination (in elements No. 5 and 6) is shown in Fig. 12, where location of maximally loaded sensors determine length of the defect.

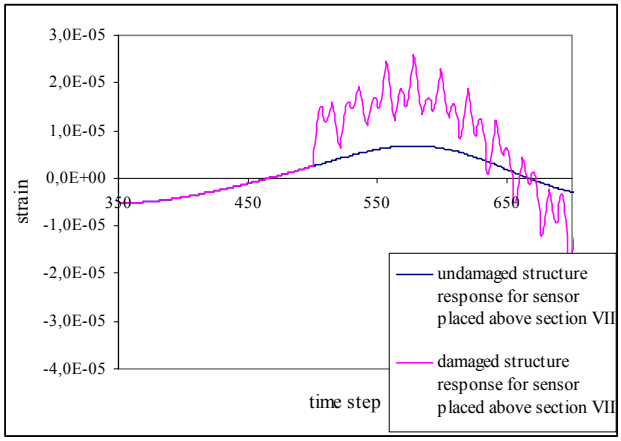

Fig.11 Responses (damaged and undamaged) for sensor placed above section VII.

a)

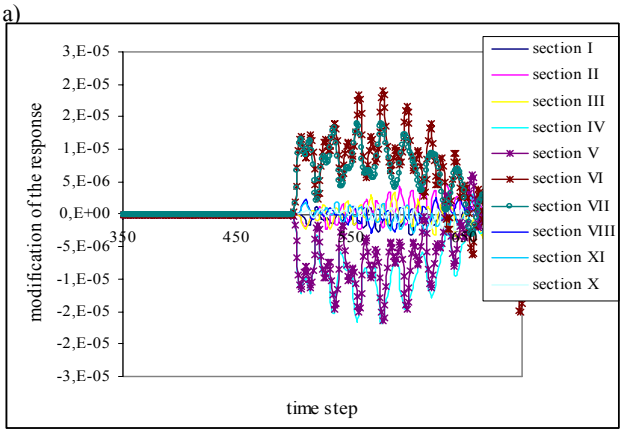

b)

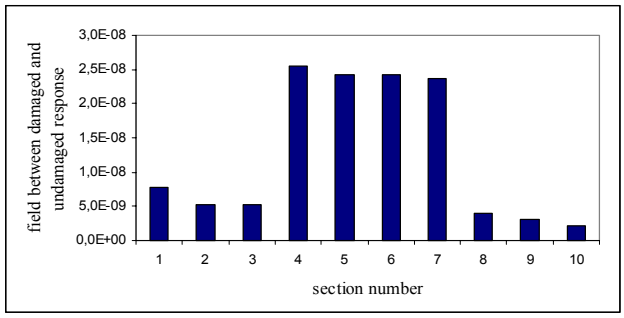

Fig. 12 a) Modification of the response due to the delamination in 5-th and 6-th section , b) field between damaged and undamaged response.

The second algorithm, making use of few sensors (e.g. in elements No.2 and 7), can be based on the VDM approach described in the previous section and solving gradient based inverse problem. More advanced applications of this proposed concept will be presented during the conference.

ACKNOWLEDGEMENT

The authors would like to gratefully acknowledge the financial support through the 5FP EU project Research Training Networks "SMART SYSTEMS" HPRN-CT-2002-00284. The work presents a part of the Ph.D. thesis of the first author, supervised by the third author.

REFERENCES

1. Rosen J. B. (1960) The Gradient Projection Method for Nonlinear Programming, Part I – Linear Constraints, *SIAM Journal of Applied Mathematics*, 8(1), pp. 181-217
2. Rosen J. B. (1961) The Gradient Projection Method for Nonlinear Programming, Part II – Nonlinear Constraints, *SIAM Journal of Applied Mathematics*, 9(4), pp. 514-532
3. Haug E. J., Arora J. S. (1979) *Applied Optimal Design: Mechanical and Structural Systems*, John Wiley & Sons, New York, U.S.A.
4. Holnicki-Szulc,J, T.Zielinski, *New damage Identification Method Through the Gradient Based Optimisation*, Proc. COST International Conference on System Identification & Structural Health Monitoring, Madrid, 6-9 Jun 2000
5. A. Orlowska, P. Kolakowski, J. Holnicki-Szulc, *Monitoring of Delamination Defects – Dynamic Case*, Proc. of the Second European Workshop Structural Health Monitoring, Munich, July 7-9, 2004